

Predictive Control Strategy for DC/AC Converters Based on Direct Power Control

Sergio Aurtenechea Larrinaga, *Student Member, IEEE*, Miguel Angel Rodríguez Vidal, *Member, IEEE*, Estanis Oyarbide, and José Ramón Torrealday Apraiz

Abstract—This paper proposes predictive direct power control (P-DPC), a new control approach where the well-known direct power control is combined with predictive selection of a voltage-vectors' sequence, obtaining both high transient dynamics and a constant-switching frequency. The developed P-DPC version is based on an optimal application of three voltage vectors in a symmetrical way, which is the so-called symmetrical 3 + 3 vectors' sequence. The simulation and experimental results of the P-DPC are compared to standard voltage-oriented control (VOC) strategies in a grid-connected three-phase voltage-source inverter under 400-V 15-kVA operation conditions. The P-DPC improves the transient response and keeps the steady-state harmonic spectrum at the same level as the VOC strategies. Due to its high transient capability and its constant-switching behavior, the P-DPC could become an interesting alternative to standard VOC techniques for grid-connected converters.

Index Terms—DC/AC power conversion, inverters, predictive control.

I. INTRODUCTION

DURING the last ten years, medium- and low-voltage grids have been interconnected to a large number of new active systems such as wind turbines, hydraulic generators, biomass and geothermal generators, photovoltaic systems, fuel cells, storage devices, and power quality improvement units (FACTS, D-FACTS, etc.). Almost all of these new installations are interconnected to the grid by means of a voltage-source inverter (VSI) and a filter [1]–[6]. Generally, these devices must provide a target active- and/or reactive-power level to the line, so appropriate power control systems are required.

This paper is focused on the control of active- and reactive-power flows of a grid-connected VSI. After a brief description of commonly used control schemes, a new control approach is

Manuscript received September 5, 2006; revised December 15, 2006. Abstract published on the Internet January 14, 2007. This work was supported in part by the programs Investigación Básica y Aplicada (PI 2003-11) and Formación de Investigadores del Departamento de Educación, Universidades e Investigación from the Basque Government and in part by MCYT DGI/FEDER under Grant ENE2005-09218-C02-00.

S. Aurtenechea Larrinaga, M. A. Rodríguez Vidal, and J. R. Torrealday Apraiz are with the Faculty of Engineering, University of Mondragon, 20500 Mondragon, Spain (e-mail: saurtenetxea@eps.mondragon.edu; marodriguez@eps.mondragon.edu; jrtorrealday@eps.mondragon.edu).

E. Oyarbide is with the Department of Electronic Engineering and Communications and Aragón Institute for Engineering Research (I3A), University of Zaragoza, 50018 Zaragoza, Spain (e-mail: eoyarbid@unizar.es).

Color versions of one or more of the figures in this paper are available online at <http://ieeexplore.ieee.org>.

Digital Object Identifier 10.1109/TIE.2007.893162

proposed: the predictive direct power control (P-DPC). Next, one of the possible control solutions of the P-DPC approach is developed. Comparative simulations and experimental results of a line-connected three-phase VSI under P-DPC and voltage-oriented control (VOC) strategies show the main advantages of the proposed control strategy.

II. INDIRECT AND DIRECT POWER CONTROL (DPC) STRATEGIES

The control techniques that are commonly used in grid-connected converter systems could be classified as direct or indirect control strategies. The indirect control is characterized by a modulator (pulsewidth modulation (PWM) or other) that computes the turn-on/turn-off times of a converter's switches along a switching period through the evaluation of the voltage reference. This voltage reference is issued by the controller, which idealizes the converter as a dependent continuous voltage source. On the other hand, direct control techniques establish a direct relation between the behavior of the controlled variable and the state of the converter's switches.

A. Indirect Power Control Techniques

VOC is a widely used indirect control strategy. It is based on the knowledge of the position of the line-voltage vector and the relative spatial orientation of the current vector [7]–[9]. It employs the well-known Park's transformation to a rotating $dq0$ reference frame aligned with the line voltage or the Clark's transformation to a static $\alpha\beta0$ reference frame.

Recent developments have popularized the virtual flux (VF) concept, which assumes that both the grid and converter's line filter behave as an ac motor. Thus, the resistance and the inductance of the filter are equivalent to the phase resistance and the leakage inductance of the motor, respectively, whereas the phase voltage of the converter is related to a fictitious VF [10], [11]. One of the main advantages of this new approach is that it is less sensitive against line-voltage variations than other approaches. The VF-oriented control (VFOC) is an adaptation of the VOC to a VF reference frame [10], [11].

Indirect control strategies generally lead to good transient behavior and acceptable steady-state operation. They operate at a constant-switching frequency, which makes the use of advanced modulation techniques possible. Thus, it becomes easier to optimize conversion power losses or simplify the line-side filter design.

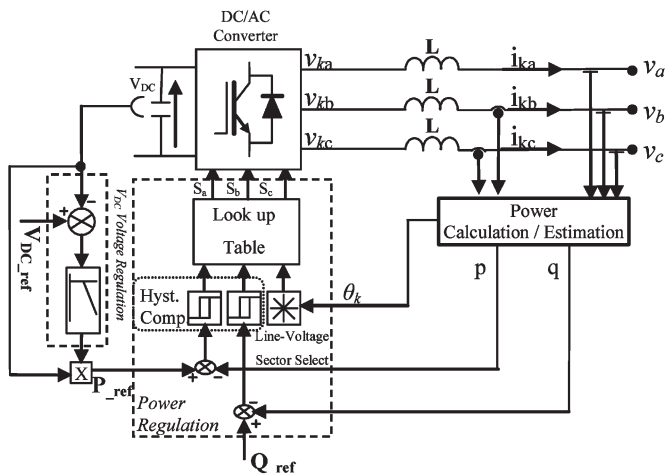


Fig. 1. Block diagram of the DPC.

However, these control techniques have some disadvantages. The main problem is common in any indirect control strategy under PWM-type modulation: if the ratio between switching and grid-fundamental frequencies is not large enough, the VSI cannot be considered as an ideal controlled continuous voltage source. In these conditions, it becomes impossible to make use of the notion of a converter's average voltage vector in control requirements.

B. DPC Techniques

DPC is one of the most popular direct control strategies of grid-connected converters [9], [11], [13]–[16]. This technique is derived from the first and original direct torque control (DTC) of ac machines. In each sampling time, it evaluates which one of the instantaneous voltage vectors (available at the output of the converter) is best suited in order to push the state of the system toward the reference value. As this evaluation is continuously carried out, the direct control technique does not require any modulator, and it is able to get the maximum dynamic capability available in the system. Moreover, it does not require any internal control loop or any coordinate transformation, avoiding coupling effects between transformed variables. In the DPC case, instantaneous active- and reactive-power control loops are based on hysteresis regulators that select the appropriate voltage vector from a lookup table (see Fig. 1).

The DPC technique has also been implanted under the VF concept, leading to the VF DPC [10], [11].

The main disadvantage of the DPC strategy is the resulting variable switching frequency, which usually is not bounded and depends mainly on the sampling time, lookup table structure, load parameters, and state of the system. Therefore, these kinds of controls generate a dispersed harmonic spectrum, making it difficult to design the line filter in order to avoid possible grid resonances [12]. The mixed DPC–space vector modulation (SVM) approach is an adaptation of VFOC and VF DPC techniques. It provides the required converter's average voltage, which is finally applied by an SVM technique [13]. This strategy could be defined as a direct control method based on the fact that converter's average voltage vector is *directly*

computed using active- and reactive-power tracking requirements. Nevertheless, in the frame of this paper and taking into consideration that it uses a modulator, it should be classified as an indirect control strategy.

Predictive approaches have also been employed in order to overcome the variable switching frequency problem of the DPC strategy. These solutions have been mainly employed in the control of ac machines [17]–[19]. Instead of selecting an instantaneous optimal voltage vector (DTC case), predictive-type approaches select an optimal set of concatenated voltage vectors, which is the so-called “voltage-vectors’ sequence.” The control problem is solved by computing the application times of the vectors of the sequence in such a way that the controlled variables converge toward the reference values along a fixed predefined switching period. In this way, constant-switching-frequency operation is obtained. Several authors have developed this concept in multilevel converter topologies linked to different kind of machines, but there are few predictive control applications on line-connected VSI systems. Some authors propose predictive current control algorithms related to power control requirements, but these works present variable switching frequencies [20], [21].

Some interesting work related to line-current control where a sliding-control-type approach is combined with a predictive computing of voltage application times has been carried out [22]. In this way, both high transient dynamics and constant-switching frequency are obtained.

Based on this idea, a new approach where DPC is combined with predictive vector sequence selection has been developed, obtaining both high transient dynamic and constant-switching frequency.

III. P-DPC THEORY AND APPLICATION TO A THREE-PHASE VSI

P-DPC selects the best voltage-vectors’ sequences and computes their application times in order to control the power flow through the VSI under a constant-switching-frequency operation. This strategy requires a predictive model of the instantaneous power behavior, which is explained next, followed by one of the possible control strategies.

A. Predictive Model of Instantaneous Power Behavior in a Line-Connected VSI

The definition of *instantaneous* active or reactive power is still a source of controversy between the researchers. Among all the theories that have been successively proposed during the last years, this work retains the “original” three-wire system’s definition [23]. Thus, instantaneous active and reactive powers are defined as follows:

$$\begin{bmatrix} P \\ Q \end{bmatrix} = \begin{bmatrix} v_\alpha & v_\beta \\ v_\beta & -v_\alpha \end{bmatrix} \begin{bmatrix} i_\alpha \\ i_\beta \end{bmatrix} \quad (1)$$

with $v_{\alpha-\beta}$ and $i_{\alpha-\beta}$ being the line voltage and current in static $\alpha\beta$ coordinates, respectively. The prediction of the power

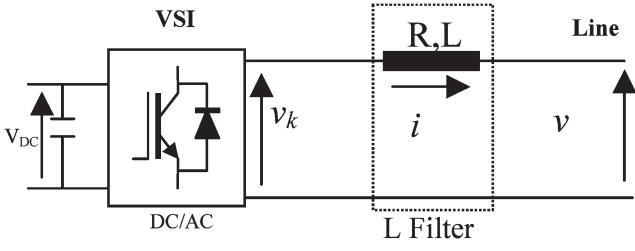


Fig. 2. One-phase model of a line-connected VSI.

behavior is based on the knowledge of the instantaneous variation of active and reactive powers, which can be expressed as

$$\begin{aligned} \frac{dP}{dt} &= v_\alpha \frac{di_\alpha}{dt} + i_\alpha \frac{dv_\alpha}{dt} + v_\beta \frac{di_\beta}{dt} + i_\beta \frac{dv_\beta}{dt} \\ \frac{dQ}{dt} &= v_\beta \frac{di_\alpha}{dt} + i_\alpha \frac{dv_\beta}{dt} - v_\alpha \frac{di_\beta}{dt} - i_\beta \frac{dv_\alpha}{dt}. \end{aligned} \quad (2)$$

The following equation shows the per-phase dynamic behavior of a VSI with an inductive filter (Fig. 2), where v_K is the converter's voltage vector, v is the line-voltage vector, and i is the line current vector:

$$v_K = Ri + L \frac{di}{dt} + v. \quad (3)$$

Neglecting the influence of the resistances of inductive elements and using Clark's transformation, the instantaneous current behavior law under static coordinates is derived, i.e.,

$$\begin{aligned} \frac{di_\alpha}{dt} &\cong \frac{1}{L}(v_{K\alpha} - v_\alpha) \\ \frac{di_\beta}{dt} &\cong \frac{1}{L}(v_{K\beta} - v_\beta). \end{aligned} \quad (4)$$

The line-voltage variation is also required in (2). Considering a nonperturbed line

$$\begin{aligned} v_\alpha &= V_S \sin(\omega t) \\ v_\beta &= -V_S \cos(\omega t) \end{aligned} \quad (5)$$

the following instantaneous line-voltage variation law is obtained:

$$\begin{aligned} \frac{dv_\alpha}{dt} &= V_S \omega \cos(\omega t) = -\omega v_\beta \\ \frac{dv_\beta}{dt} &= V_S \omega \sin(\omega t) = \omega v_\alpha. \end{aligned} \quad (6)$$

Replacing (4) and (6) in (2), functions describing instantaneous active- and reactive-power time-derivative behaviors are obtained, i.e.,

$$\begin{aligned} \frac{dP}{dt} &= v_\alpha \left(\frac{1}{L}(v_{K\alpha} - v_\alpha) + \omega i_\beta \right) + v_\beta \left(\frac{1}{L}(v_{K\beta} - v_\beta) - \omega i_\alpha \right) \\ \frac{dQ}{dt} &= v_\alpha \left(\omega i_\alpha - \frac{1}{L}(v_{K\beta} - v_\beta) \right) + v_\beta \left(\frac{1}{L}(v_{K\alpha} - v_\alpha) + \omega i_\beta \right). \end{aligned} \quad (7)$$

Analyzing (7), it can be deduced that the power time-derivative values depend on the grid parameters, filter inductors, and the converter's switching state. Fig. 3 shows, under unity-power-factor steady-state operation, the behavior of seven different slopes, which are related to the available seven voltage-vectors. Any given voltage $v_k = [v_{k\alpha} \ v_{k\beta}]^T$ at the output of the VSI is kept constant during each voltage-vector application. In the same way, if the switching frequency is high enough, the line voltage $v = [v_\alpha \ v_\beta]^T$ can also be considered as a constant value during the same period. Thus, and provided that current variations are small, quasi-constant active- and reactive-power slopes can be considered during each voltage-vector application. These assumptions allow simple geometrical analysis of concatenated power behaviors. Active- and reactive-power-expression slopes during a voltage-vector application are defined as follows:

$$\begin{aligned} f_{pi} &= \frac{dP}{dt} \Big|_{\vec{V}_k = \vec{V}_i} \\ f_{qi} &= \frac{dQ}{dt} \Big|_{\vec{V}_k = \vec{V}_i} \end{aligned} \quad (8)$$

with i denoting the position index of the applied voltage in the sequence of voltage-vectors. Equation (9) computes the linear trajectories of active and reactive powers under a given voltage-vector application during the related application time, i.e.,

$$\begin{aligned} P_i &= P_{i-1} + f_{pi} t_{ai} \\ Q_i &= Q_{i-1} + f_{qi} t_{ai} \end{aligned} \quad (9)$$

where $\{P_{i-1} \ Q_{i-1}\}$ are the initial active- and reactive-power values in the beginning of the i th vector of the sequence, t_{ai} is the application time, and $\{P_i \ Q_i\}$ are the active- and reactive-power values at the end of the application time.

B. P-DPC Based on a Symmetrical 3 + 3 Vectors' Sequence

The P-DPC strategy is based on the concatenation of several (9)-type trajectories along the control period, leading to the so-called voltage-vectors' sequence. This concatenation can be carried out in different ways, e.g., it can result in a nonsymmetrical switching pattern containing two or three voltage vectors or it can provide a symmetrical switching pattern combining two or three vectors, which are the so-called 2 + 2 or 3 + 3 voltage-vectors' sequences [24].

This paper deals with the symmetrical 3 + 3 switching pattern example where the voltage-vectors' sequence is divided into two subsequences of three voltage vectors each (see Fig. 4). The second subsequence is symmetrical to the first one, i.e., it employs the same voltage vectors and application times but reverses the application order. Thus, the last voltage vector of the first sequence matches up with the first voltage vector of the second sequence, leading to a switching frequency minimization. Fig. 4 shows an example of the concatenation of power-trajectories with the first steady-state control period followed by a reference transient response. In the beginning of each control period, the algorithm must select three of the applicable

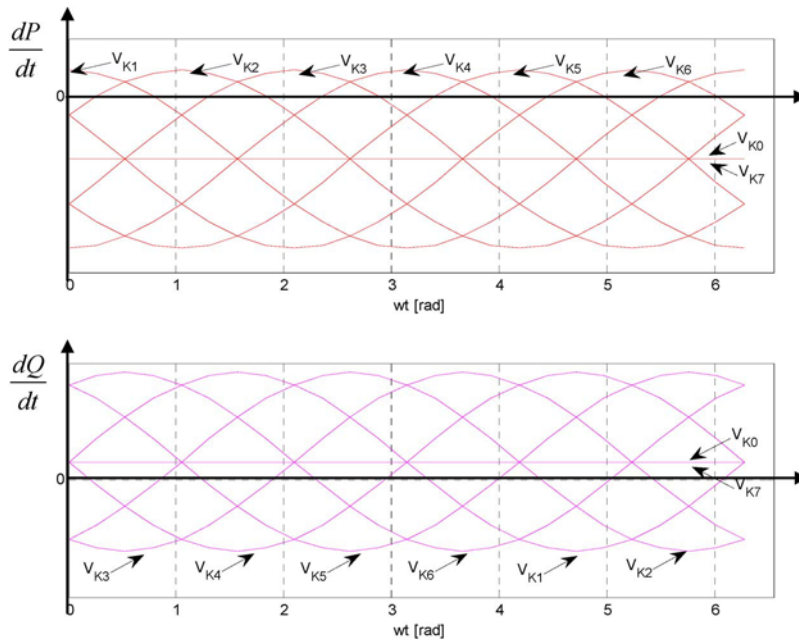


Fig. 3. Active- and reactive-power time-derivative behaviors under unity-power-factor steady-state operation.

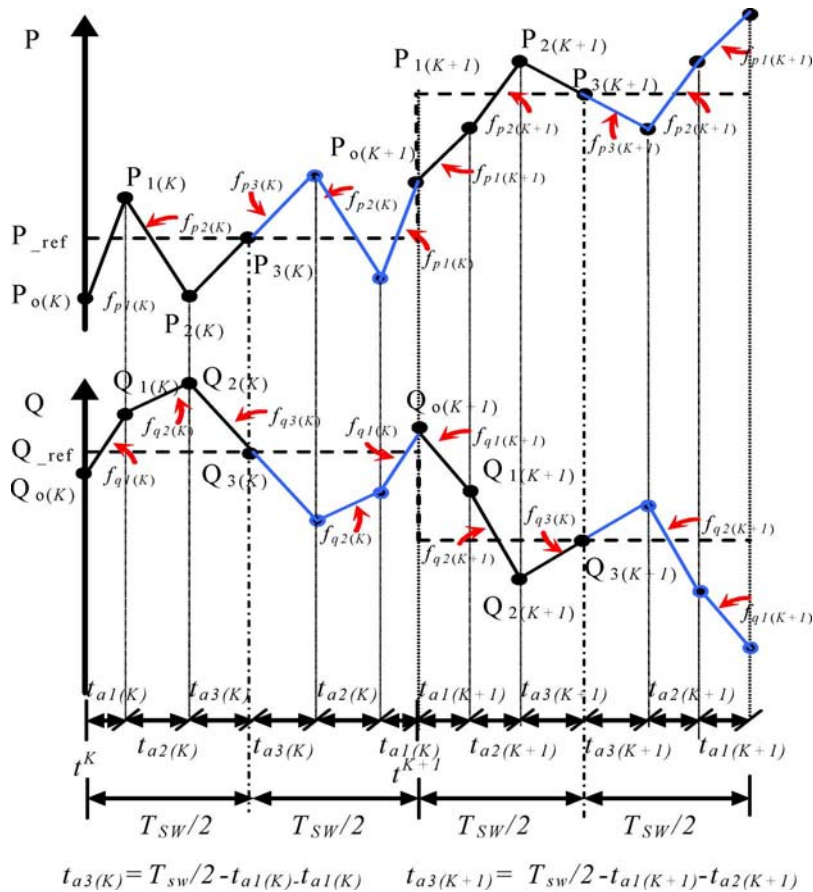


Fig. 4. Example of the steady-state and transient behavior of the P-DPC strategy with a 3 + 3 symmetrical voltage-vectors sequence.

voltage vectors, followed by the computation of the required application times.

1) *Voltage-Vectors' Selection:* Among other optimization criteria, it is usual to reduce the number of commutations and, with it, the power losses of semiconductors. Therefore, the

basic idea of the minimum loss vector PWM (MLV-PWM) could be of interest [25]. The voltage-vectors' sequence is chosen in such a way that the switching of a VSI leg does not happen during the line-current maximum, leading to minimum switching losses.

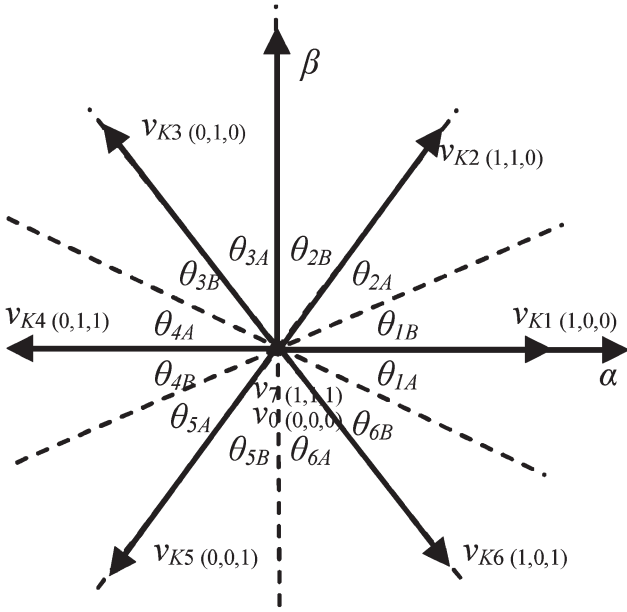


Fig. 5. Set of available voltage vectors on a three-phase converter and mapping of the segments related to the line-voltage vector location.

The line-voltage plane is divided into six sectors of 60° $[\theta_1, \dots, \theta_6]$, which are also divided into two subsectors, $[\theta_{iA}, \dots, \theta_{iB}]$ (see Fig. 5). As the use of the nearest voltage vectors provides the smallest current ripple, when the grid voltage is located at any given sector θ_i , each voltage application subsequence must be built by active voltage vectors belonging to the set $\{\vec{v}_i, \vec{v}_{i-1}, \vec{v}_{i+1}\}$ and by one of the two null vectors $\{\vec{v}_0, \vec{v}_7\}$. In the first sector case, for example, the following voltage application subsequences can be used:

$$\{[\vec{v}_1, \vec{v}_6, \vec{v}_7], [\vec{v}_1, \vec{v}_2, \vec{v}_7], [\vec{v}_7, \vec{v}_6, \vec{v}_1], [\vec{v}_7, \vec{v}_2, \vec{v}_1]\}. \quad (10)$$

The last two subsequences are symmetrical to the previous ones. The appropriate vectors' sequence will depend on the involved subsector and the switching-losses optimization strategy [25].

2) *Application Times*: Equation (9), combined with the constant-switching frequency constraint, form the set of equations defining the overall behavior of active and reactive powers during the voltage-vectors' sequence, i.e.,

$$\begin{aligned} P_1 &= P_0 + f_{p1} \cdot 2t_{a1} & / & & Q_1 &= Q_0 + f_{q1} \cdot 2t_{a1} \\ P_2 &= P_1 + f_{p2} \cdot 2t_{a2} & / & & Q_2 &= Q_1 + f_{q2} \cdot 2t_{a2} \\ P_3 &= P_2 + f_{p3} \cdot 2t_{a3} & / & & Q_3 &= Q_2 + f_{q3} \cdot 2t_{a3} \\ T_{sw}/2 &= t_{a1} + t_{a2} + t_{a3}. \end{aligned} \quad (11)$$

The control algorithm must compute the application times $\{t_{a1}, t_{a2}, t_{a3}\}$ in such a way that controlled variables evolve from their initial values $\{P_0, Q_0\}$ toward the reference values $\{P_3, Q_3\}$. The problem has seven equations and six variables, so an approximate solution based on some optimization criteria must be computed. The selected approach tries to minimize the active- and reactive-power tracking errors, which are defined as

$$\begin{aligned} e_{Fp} &= \overbrace{P_{ref} - P_0}^{e_{po}} - 2f_{p1}t_{a1} - 2f_{p2}t_{a2} \\ &\quad - 2f_{p3} \left(\frac{T_{sw}}{2} - t_{a1} - t_{a2} \right) \\ e_{Fq} &= \overbrace{Q_{ref} - Q_0}^{e_{qo}} - 2f_{q1}t_{a1} - 2f_{q2}t_{a2} \\ &\quad - 2f_{q3} \left(\frac{T_{sw}}{2} - t_{a1} - t_{a2} \right). \end{aligned} \quad (12)$$

A least-square optimization method is used, trying to minimize the weight function of

$$F = e_{Fp}^2 + e_{Fq}^2. \quad (13)$$

The optimal set of application times that minimizes F during a control period satisfies the following two minimum value conditions:

$$\begin{cases} \frac{\partial F}{\partial t_{a1}} = 0 \\ \frac{\partial F}{\partial t_{a2}} = 0 \end{cases}. \quad (14)$$

Having solved the set of equations derived from (14), it is straightforward to get (15), shown at the bottom of the page (see the Appendix).

C. Proposed Control System Configuration

The system's block diagram and the flowchart of the proposed P-DPC technique are shown in Fig. 6. Initial line-voltage and line-current values are required in order to compute the initial active and reactive powers $[P_0, Q_0]$. The proposed strategy evaluates this information and the reference power values, selects the appropriate sequence (trying to minimize the line-current ripple), and computes the application times, which minimize the final tracking errors.

$$\begin{aligned} t_{a1} &= \frac{[(f_{q2} - f_{q3}) \cdot e_{po} + (f_{p3} - f_{p2}) \cdot e_{qo} + (f_{q3} \cdot f_{p2} - f_{q2} \cdot f_{p3}) \cdot \frac{T_{sw}}{2}]}{[f_{q3} \cdot f_{p2} - f_{q1} \cdot f_{p2} - f_{q2} \cdot f_{p3} + f_{q1} \cdot f_{p3} - f_{q3} \cdot f_{p1} + f_{q2} \cdot f_{p1}]} \\ t_{a2} &= \frac{[(f_{q3} - f_{q1}) \cdot e_{po} + (f_{p1} - f_{p3}) \cdot e_{qo} + (-f_{q3} \cdot f_{p1} + f_{q1} \cdot f_{p3}) \cdot \frac{T_{sw}}{2}]}{[f_{q3} \cdot f_{p2} - f_{q1} \cdot f_{p2} - f_{q2} \cdot f_{p3} + f_{q1} \cdot f_{p3} - f_{q3} \cdot f_{p1} + f_{q2} \cdot f_{p1}]} \\ t_{a3} &= \frac{T_{sw}}{2} - t_{a1} - t_{a2} \end{aligned} \quad (15)$$

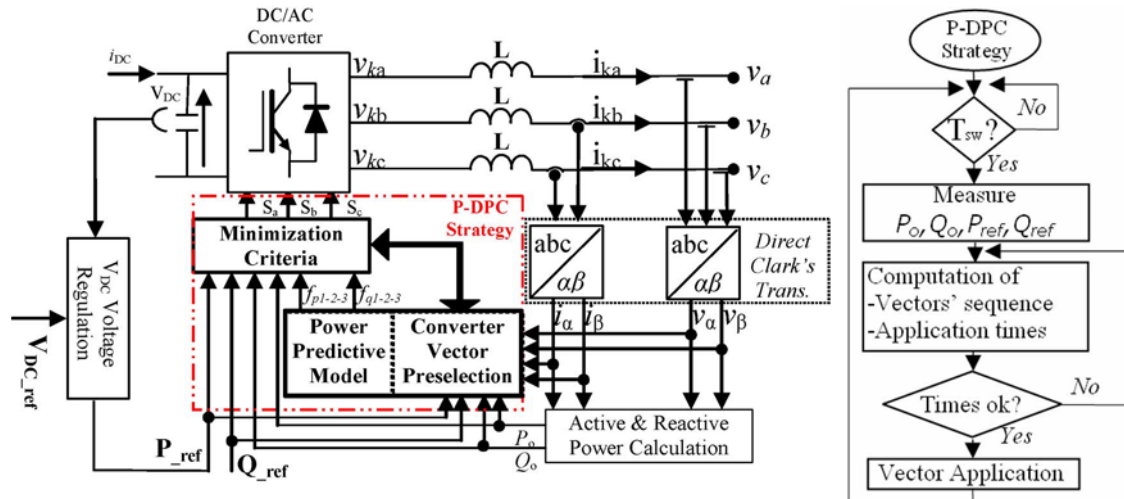


Fig. 6. System's block diagram and control flowchart of the P-DPC strategy.

TABLE I
SPECIFICATIONS OF THE GRID-CONNECTED THREE-PHASE VSI

	Value [unit]
Rated Power	15 [kVA] $\cos\theta=0.8(i)$
Rated line-to-line Voltage	400 [V]
Filter (L)	10 [mH] $\pm 10\%$
DC Link (C_{DC})	5 [mF] / 700 [V]
Control Period T_{SW}	500 [μ s]

IV. SIMULATION AND EXPERIMENTAL RESULTS

In order to verify the behavior of the proposed control algorithm, comparative simulations and experimental tests have been carried out, comparing two VOC-type strategies (both symmetrical space vector PWM (SV-PWM) and MLV-PWM) to the proposed P-DPC strategy. The specifications and parameters of the model are listed in Table I.

A. Simulation Results

Fig. 7 shows the resulting per-phase switching signals and normalized per-phase current. It can be observed that, in the MLV-PWM and P-DPC cases, there are no switching actions along the maximum of the line-current, minimizing the overall switching losses. However, this efficiency improvement is related to current-spectrum deterioration, as will be shown later.

The best P-DPC result is obtained, as expected, in transient behavior (see Fig. 8). Two steps of active- and reactive-power references from 0 to 15 kW and 9 kVAR, respectively, have been applied. Though the P-DPC offers a slight improvement on reactive-power transient, it is clearly faster in the active-power tracking task, as it takes less than 5 ms against the 60 ms required by either of the two VOC strategies.

On the other hand, detailed behaviors of variables under P-DPC are shown in Fig. 9. Two control periods are represented. As it can be observed, quasi-linear active- and reactive-

power trajectories evolve around the reference values, with a ripple of about 5%.

B. Experimental Results

Some experimental tests have been carried out in order to validate the retained approach. The experimental platform is located in the Power Electronics Laboratory, Faculty of Engineering, University of Mondragón.

In the beginning of each control period, the control computes active and reactive powers based on the instantaneous current and voltage measures. Then, the P-DPC algorithm selects the optimum voltage-vectors' sequence and the related application times, taking into account the power tracking requirements. The control task takes less than 5 μ s, which is negligible against to the control period (500 μ s). After this short delay time, the selected voltage vectors are applied during the computed application times, completing the control period. The control algorithm (instantaneous power derivation, vectors' sequence selection, and application times calculation) runs under the SIMULINK/MATLAB environment in a dSPACE ds1103 real-time platform. As the SVM facility of this platform is not flexible enough, the desired switching patterns are "coded" using scalar PWM facilities. The desired actual voltage-vector sequence is finally generated, "decoding" these standard PWM outputs by combinatory logic circuits. The measurement system is based on a Yokogawa PZ4000 device whose sample time is 250 kS/s.

Fig. 10 compares the transient behaviors of the three control strategies when an active-power reference step is applied. As it can be observed, the P-DPC transient takes only 5 ms, whereas the VOC-based strategies need about 60 ms to achieve the same transient. Fig. 11 reflects the active- and reactive-power trajectories of two symmetrical 3 + 3 switching sequences. These variables evolve in a quasi-linear way around the reference values.

Steady-state performance is evaluated by total harmonic distortion (THD) measurements (see Fig. 12). The VOC-type SV-PWM strategy shows the best power quality ($THD_i = 4.10\%$),

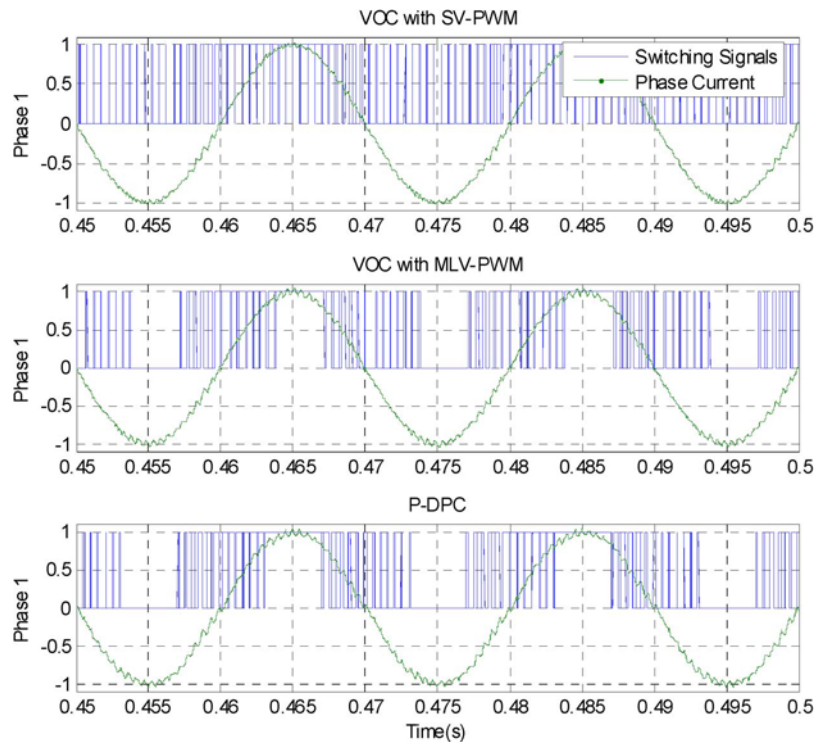


Fig. 7. Simulated per-unit phase switching signals and current behaviors in steady-state operation.

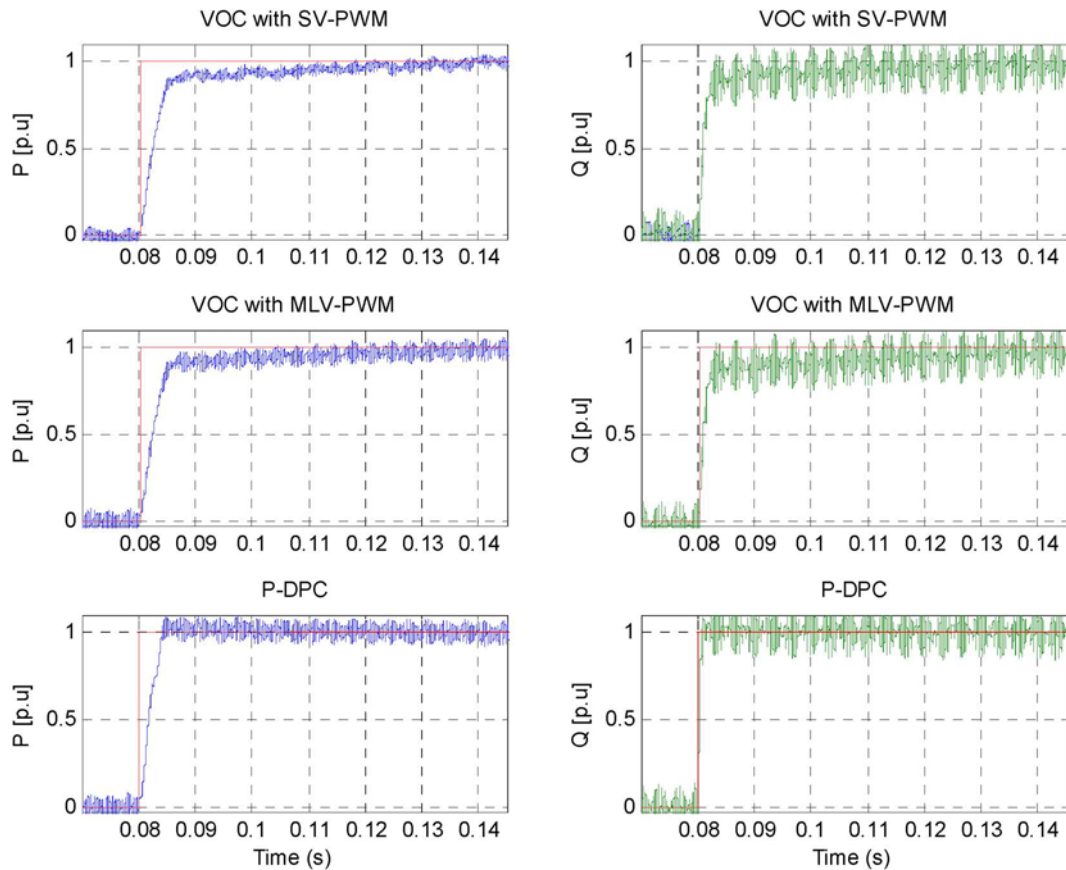


Fig. 8. Simulated instantaneous power behavior during active- and reactive-power-reference steps.

followed by the P-DPC ($THD_i = 4.84\%$) and the VOC-based MLV-PWM ($THD_i = 4.86\%$). As explained previously, both the P-DPC and MLV-PWM approaches minimize the switching

losses with the same vector selection strategy, which leads naturally to a similar THD degradation. This THD penalization is an expected result, considering that some degrees of freedom

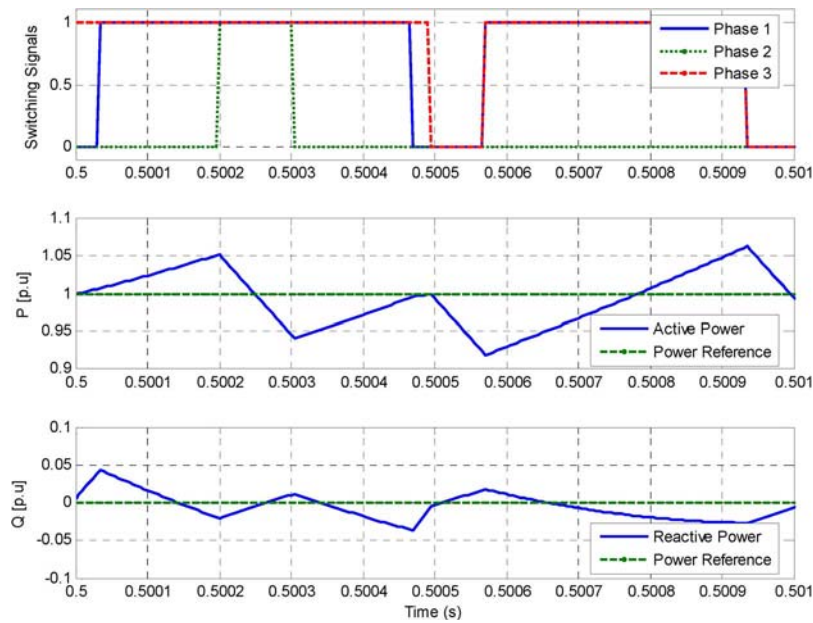


Fig. 9. Simulated switching signals and active- and reactive-power trajectories along two control periods.

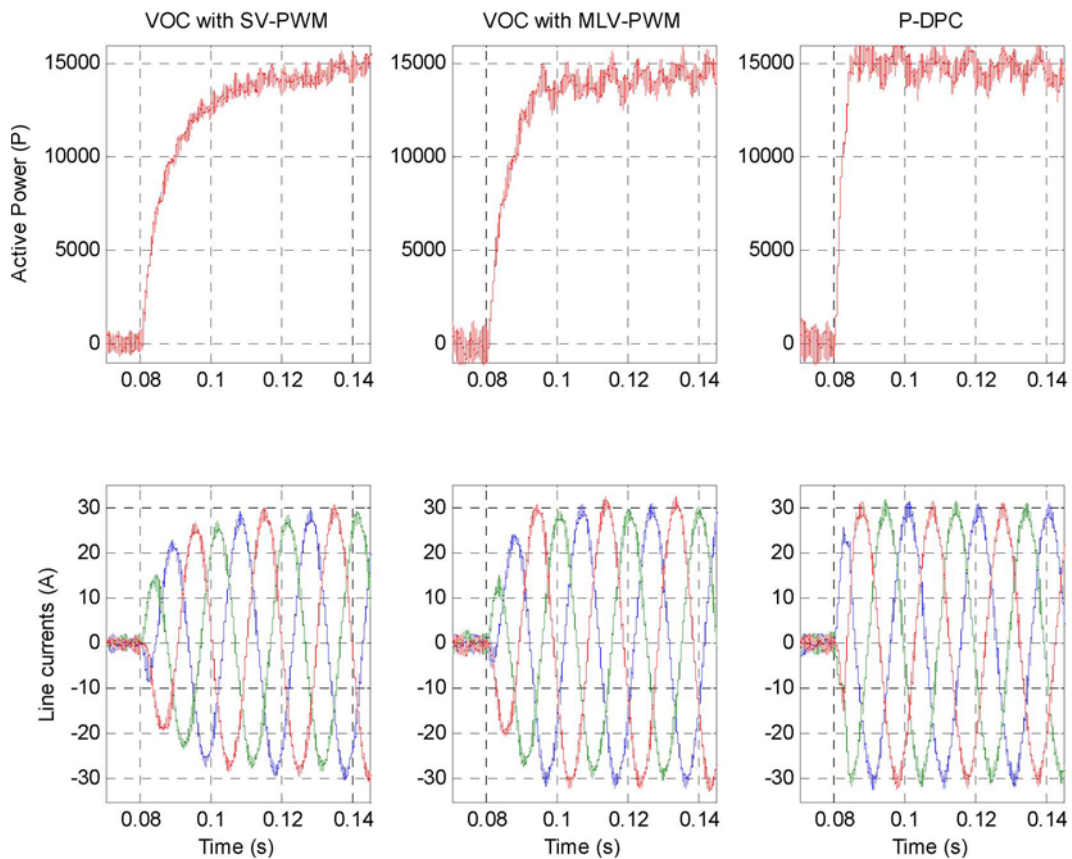


Fig. 10. Experimental instantaneous active power and line-current behavior during an active-power reference step.

are not used in current control tasks. Nevertheless, all strategies meet the IEEE Std. 519-1992 recommendation.

V. CONCLUSION

A new predictive-type DPC strategy (P-DPC) is proposed. Due to this new approach, constant-switching-frequency oper-

ation is obtained, keeping the fast dynamic response related to direct control strategies.

The new control approach has been compared to VOC-based SV-PWM and MLV-PWM strategies, showing that the P-DPC is several times faster in active-power reference transients. It offers the same power-loss reduction than the MLV-PWM, and therefore, the resulting THD is also penalized. Nevertheless,

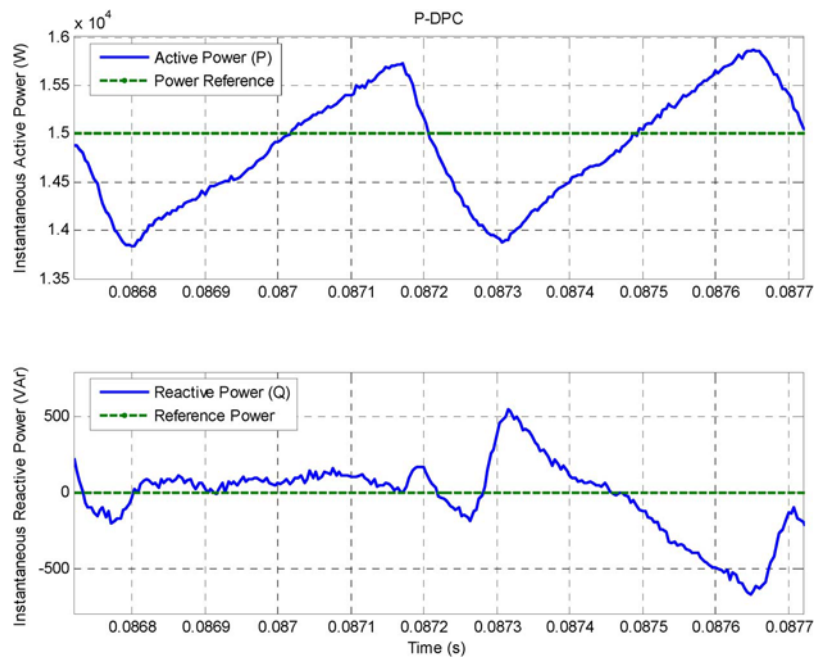


Fig. 11. Experimental active- and reactive-power trajectories along two control periods.

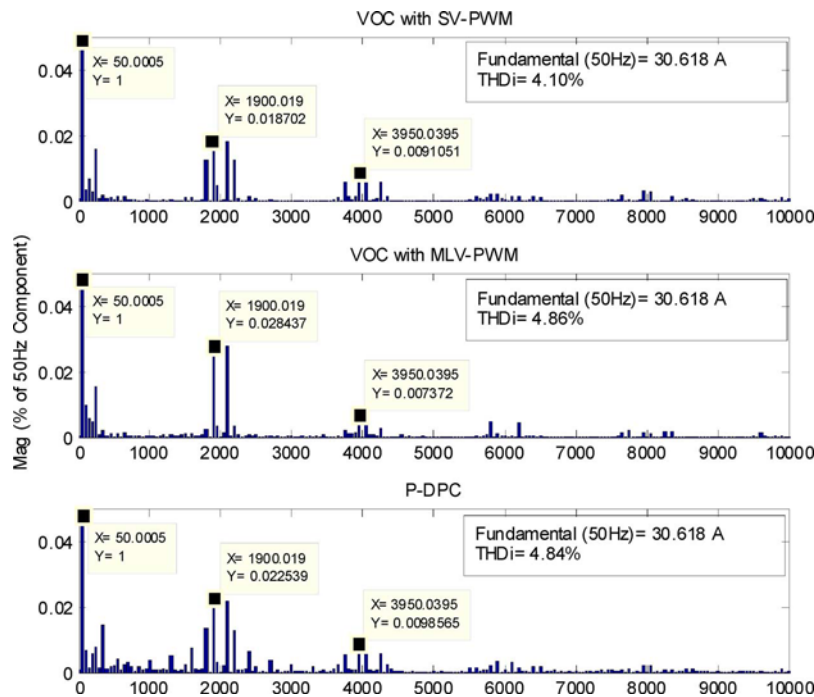


Fig. 12. Experimental current-frequency spectrum.

all control strategies analyzed in this paper meet the IEEE Std. 519-1992 recommendation.

Important P-DPC improvements are possible. This is the case of the selection of active voltage vectors. The proposed strategy selects the nearest active voltage vectors improving the steady-state performance. Obviously, this is not the best strategy for transients, where other far active voltage vectors would provide faster response. In a similar way, this mathematical approach is based on the knowledge of the system’s model, and therefore,

it is sensitive to parameter drifts. A typical deviation of 10% in the filter’s inductance value will produce little errors below 10% in the resulting application times, so it will not damage the stability of the control system. Anyway, the resulting nonexpected error could be utilized in an online parameter’s estimation system, leading to an adaptive P-DPC.

As a general conclusion, the P-DPC approach could become an interesting alternative to VOC techniques for line-connected converters.

$$\begin{cases} \frac{dF}{dt_{a1}} = 2(e_{p0} - 2f_{p1}t_{a1} - 2f_{p2}t_{a2} - 2f_{p3}(\frac{1}{2}T_{sw} - t_{a1} - t_{a2}))(-2f_{p1} + 2f_{p3}) \\ \quad + 2(e_{q0} - 2f_{q1}t_{a1} - 2f_{q2}t_{a2} - 2f_{q3}(\frac{1}{2}T_{sw} - t_{a1} - t_{a2}))(-2f_{q1} + 2f_{q3}) = 0 \\ \frac{dF}{dt_{a2}} = 2(e_{p0} - 2f_{p1}t_{a1} - 2f_{p2}t_{a2} - 2f_{p3}(\frac{1}{2}T_{sw} - t_{a1} - t_{a2}))(-2f_{p2} + 2f_{p3}) \\ \quad + 2(e_{q0} - 2f_{q1}t_{a1} - 2f_{q2}t_{a2} - 2f_{q3}(\frac{1}{2}T_{sw} - t_{a1} - t_{a2}))(-2f_{q2} + 2f_{q3}) = 0 \end{cases} \quad (17)$$

APPENDIX

Having combined (12) in (13), we get the weight function of the form

$$F = f(t_{a1}, t_{a2}). \quad (16)$$

The sensitivity of this function against t_{a1} and t_{a2} is shown in (17), at the top of the page.

We get the minimum of F when the values of the two sensitivity functions equal zero. The resulting set of two equations and two variables can be easily computed, leading to the solution shown in (15).

REFERENCES

- [1] S. Bernet, "State of the art and developments of medium voltage converters," in *Proc. PELINCEC*, Warsaw, Poland, 2005, pp. 1–11.
- [2] F. Blaabjerg, T. Teodorescu, M. Liserre, and A. V. Timbus, "Overview of control and grid synchronization for distributed power generation systems," *IEEE Trans. Ind. Electron.*, vol. 53, no. 5, pp. 1398–1409, Oct. 2006.
- [3] S. Alepuz, S. Busquets-Monge, J. Bordonau, J. Gago, D. González, and J. Balcells, "Interfacing renewable energy sources to the utility grid using a three-level inverter," *IEEE Trans. Ind. Electron.*, vol. 53, no. 5, pp. 1504–1511, Oct. 2006.
- [4] D. M. Vilathgamuwa, P. C. Loh, and Y. Li, "Protection of microgrids during utility voltage sags," *IEEE Trans. Ind. Electron.*, vol. 53, no. 5, pp. 1427–1436, Oct. 2006.
- [5] J. M. Guerrero, J. Matas, L. Garcia De Vicuna, M. Castilla, and J. Miret, "Wireless-control strategy for parallel operation of distributed-generation," *IEEE Trans. Ind. Electron.*, vol. 53, no. 5, pp. 1461–1470, Oct. 2006.
- [6] M. Prodanovic and T. C. Green, "High-quality power generation through distributed control of a power park microgrid," *IEEE Trans. Ind. Electron.*, vol. 53, no. 5, pp. 1471–1482, Oct. 2006.
- [7] R. Rocha and L. de Siqueira Martins, "A discrete current control for PWM rectifier," in *Proc. ISIE*, 2005, pp. 681–686.
- [8] M. Salo and H. Tuusa, "A vector-controlled PWM current-source-inverter-fed induction motor drive with a new stator current control method," *IEEE Trans. Ind. Electron.*, vol. 52, no. 2, pp. 523–531, Apr. 2005.
- [9] J. Salomaki, M. Hinkkanen, and J. Luomi, "Sensorless control of induction motor drives equipped with inverter output filter," *IEEE Trans. Ind. Electron.*, vol. 53, no. 4, pp. 1188–1197, Jun. 2006.
- [10] M. Malinowski, "Sensorless control strategies for three-phase PWM rectifiers," Ph.D. dissertation, Faculty Elect. Eng., Inst. Control Ind. Electron., Warsaw, Poland, 2001.
- [11] M. Malinowski, M. P. Kazmierkowski, and A. M. Trzynadlowski, "A comparative study of control techniques for PWM rectifiers in ac adjustable speed drives," *IEEE Trans. Power Electron.*, vol. 18, no. 6, pp. 1390–1396, Nov. 2003.
- [12] R. L. Kirlin, M. M. Bech, and A. M. Trzynadlowski, "Analysis of power and power spectral density in PWM inverters with randomized switching frequency," *IEEE Trans. Ind. Electron.*, vol. 49, no. 2, pp. 486–499, Apr. 2002.
- [13] M. P. Kazmierkowski, R. Krishnan, and F. Blaabjerg, *Control in Power Electronics*. New York: Academic, 2002.
- [14] G. Escobar, A. M. Stanković, J. M. Carrasco, E. Galván, and R. Ortega, "Analysis and design of direct power control (DPC) for a three phase synchronous rectifier via output regulation subspaces," *IEEE Trans. Power Electron.*, vol. 18, no. 3, pp. 823–830, May 2003.
- [15] T. Noguchi, H. Tomiki, S. Kondo, and I. Takahashi, "Direct power control of PWM converter without power-source voltage sensors," *IEEE Trans. Ind. Appl.*, vol. 34, no. 3, pp. 473–479, May/Jun. 1998.
- [16] S. Chen and G. Joós, "Direct power control of active filters with averaged switching frequency regulation," in *Proc. IEEE PESC*, 2004, pp. 1187–1194.
- [17] A. Linder and R. Kennel, "Direct model predictive control—A new direct predictive control strategy for electrical drives," in *Proc. EPE*, Dresden, Germany, 2005, pp. 1–10.
- [18] A. Ben Abdelghani, C. A. Martins, X. Roboam, and T. A. Meynard, "Use of extra degrees of freedom in multilevel drives," *IEEE Trans. Ind. Electron.*, vol. 49, no. 5, pp. 965–977, Oct. 2002.
- [19] M. Pacas and J. Weber, "Predictive direct torque for the PM synchronous machine," *IEEE Trans. Ind. Electron.*, vol. 52, no. 5, pp. 1350–1356, Oct. 2005.
- [20] P. Antoniewicz, "Predictive direct power control of a rectifier," in *Proc. PELINCEC*, Warsaw, Poland, 2005, pp. 1–3.
- [21] J. Rodríguez, J. Pontt, P. Corea, U. Ammann, and P. Cortés, "Novel control strategy of an ac/dc/ac converter using power relations," in *Proc. PELINCEC*, Warsaw, Poland, 2005, pp. 1–6.
- [22] A. Sariñana, S. Guffon, G. Bornard, and S. Bacha, "A novel fixed switching frequency controller of a three-phase voltage source inverter," in *Proc. EPE*, Lausanne, Switzerland, 1999, pp. 1–9.
- [23] H. Akagi, Y. Kanazawa, and A. Nabae, "Instantaneous reactive power compensators comprising switching devices without energy storage components," *IEEE Trans. Ind. Appl.*, vol. 20, no. 3, pp. 625–630, May/Jun. 1984.
- [24] S. Aurtenechea, M. A. Rodríguez, E. Oyarbide, and J. R. Torrealday, "Predictive direct power control—A new control strategy for dc/ac converters," in *Proc. IEEE IECON*, Paris, France, 2006, pp. 1661–1666.
- [25] A. M. Trzynadlowski and S. Legowski, "Minimum-loss vector strategy for three phase inverters," *IEEE Trans. Power Electron.*, vol. 9, no. 1, pp. 26–34, Jan. 1994.



Sergio Aurtenechea Larrinaga (S'04) was born in Guernica, Spain, on January 18, 1977. He received the B.Eng. degree from the Escuela de Ingeniería Técnica Industrial de Eibar, Eibar, Spain, in 2000, and the M.Eng. degree from the University of Mondragon, Mondragon, Spain, in 2003. He is currently working toward the Ph.D. degree at the University of Mondragon.

His research is focused on the analysis, design, and control of high-power converters, especially when they are employed for grid-connected systems.



Miguel Angel Rodríguez Vidal (M'06) was born in San Sebastian, Spain, in August 1966. He received the B.Sc. degree in electrical engineering from the Swiss Federal Institute of Technology, Lausanne, Switzerland, in 1992, and the Ph.D. degree in industrial engineering from the University of Zaragoza, Zaragoza, Spain, in 2000.

In 1992, he joined the Department of Electronics, Faculty of Engineering, University of Mondragon, Mondragon, Spain, where he is currently an Associate Professor. He has participated in different research projects in the field of wind energy systems, lift drives, and railway traction. His research interests include electrical machines modeling and control, in particular, for single- and doubly-fed asynchronous machines, and voltage-source-inverter control.



Estanis Oyarbide was born in Beasain, Spain, on June 30, 1969. He received the B.Eng. degree from the University of Mondragon, Mondragon, Spain, in 1992, and the M.Eng. and Ph.D. degrees from the National Polytechnic Institute of Grenoble, Grenoble, France, in 1994 and 1998, respectively.

From 1998 to 2002, he was a Lecturer in the Department of Electronics, University of Mondragon, specializing in power converters and adjustable-speed drives. He is currently an Assistant Lecturer in the Department of Electronic Engineering and

Communications and a Researcher at the Aragon Institute for Engineering Research (I3A), both at the University of Zaragoza, Zaragoza, Spain, which he joined in 2002. His current research interests include the control of static high-power converters in wind-turbine applications.



José Ramón Torrealday Apraiz was born in Guernica, Spain, in February 1944. He received the B.Sc. and Ph.D. degrees in electronics from the University of the Basque Country, Bilbao, Spain, in 1968 and 1983, respectively.

In 1969, he joined the Department of Electronics, Faculty of Engineering, University of Mondragon, Mondragon, Spain, where he is currently the Head of the department. He has been involved in different research projects in the field of variable-frequency ac motor drive systems and interconnection of renew-

able energy sources to the utility grid. His current research interests include power electronic converters for electrical drives and power quality.